NME 2176 pp: 1–23 (col.fig.: Jil) PROD. TYPE: COM ED: Usha PAGN: Padmashini – SCAN: Nil

INTERNATIONAL JOURNAL FOR NUMERICAL METHODS IN ENGINEERING
Int. J. Numer. Meth. Engng (2007)
Published online in Wiley InterScience (www.interscience.wiley.com). DOI: 10.1002/nme.2176

Unique real-variable expressions of displacement and traction fundamental solutions covering all transversely isotropic elastic materials for 3D BEM

L. Távara, J. E. Ortiz, V. Mantič*, † and F. París

School of Engineering, University of Seville, Camino de los Descubrimientos s/n, Sevilla E-41092, Spain

SUMMARY

A general, efficient and robust boundary element method (BEM) formulation for the numerical solution of three-dimensional linear elastic problems in transversely isotropic solids is developed in the present work. The BEM formulation is based on the closed-form real-variable expressions of the fundamental solution in displacements U_{ik} and in tractions T_{ik}, originated by a unit point force, valid for any combination of material properties and for any orientation of the radius vector between the source and field points. A compact expression of this kind for U_{ik} was introduced by Ting and Lee (*Q. J. Mech. Appl. Math.* 1997; **50**:407–426) in terms of the Stroh eigenvalues on the oblique plane normal to the radius vector. Working from this expression of U_{ik}, and after a revision of their final formula, a new approach (based on the application of the rotational symmetry of the material) for deducing the derivative kernel $U_{ik,j}$ and the corresponding stress kernel Σ_{ijk} and traction kernel T_{ik} has been developed in the present work. These expressions of U_{ik}, $U_{ik,j}$, Σ_{ijk} and T_{ik} do not suffer from the difficulties of some previous expressions, obtained by other authors in different ways, with complex-valued functions appearing for some combinations of material parameters and/or with division by zero for the radius vector at the rotational-symmetry axis. The expressions of U_{ik}, $U_{ik,j}$, Σ_{ijk} and T_{ik} have been presented in a form suitable for an efficient computational implementation. The correctness of these expressions and of their implementation in a three-dimensional collocational BEM code has been tested numerically by solving problems with known analytical solutions for different classes of transversely isotropic materials. Copyright © 2007 John Wiley & Sons, Ltd.

Received 13 March 2007; Revised 20 July 2007; Accepted 24 July 2007

KEY WORDS: linear elasticity; transversely isotropic material; fundamental solution; free-space Green's function; boundary integral equation; boundary element method

*Correspondence to: V. Mantič, School of Engineering, University of Seville, Camino de los Descubrimientos s/n, Sevilla E-41092, Spain.

†E-mail: mantic@esi.us.es, mantic@supercable.es

Contract/grant sponsor: Junta de Andalucia; contract/grant number: TEP 1207
Contract/grant sponsor: Spanish Ministry of Education and Science; contract/grant number: TRA2005-06764

1. INTRODUCTION

An accurate and efficient evaluation of the integral kernels, typically represented by a *fundamental solution* (*free-space Green's function*) and its derivatives, is a key issue in the numerical solution of boundary integral equations (BIEs) by the boundary element method (BEM) [1–3], the method of fundamental solutions [4] and other approaches.

Consider a homogeneous linearly elastic anisotropic material characterized by the fourth rank tensor of elastic stiffnesses $C_{ijk\ell}$ $(i, j, k, \ell = 1, 2, 3)$, verifying the symmetry relations $C_{ijk\ell} = C_{jik\ell} = C_{k\ell ij}$. Then, the constitutive law can be written as

$$\sigma_{ij}(\mathbf{x}) = C_{ijk\ell}\varepsilon_{k\ell}(\mathbf{x}) = C_{ijk\ell}u_{k,\ell}(\mathbf{x}) \tag{1}$$

where σ_{ij}, $\varepsilon_{k\ell}$ and u_k, are respectively, the tensors of stresses and strains and the vector of displacements at a point $\mathbf{x} = (x_1, x_2, x_3)$. It is assumed that $C_{ijk\ell}$ is a positive-definite tensor, i.e. $C_{ijk\ell}\varepsilon_{ij}\varepsilon_{k\ell} > 0$ for any non-zero strain tensor.

Let $\mathbf{U}(\mathbf{x})$ denote a fundamental solution for the above material given by a 3×3 matrix whose columns represent displacement vectors (at a point $\mathbf{x} \neq \mathbf{0}$) originated in the infinite anisotropic elastic medium ($\mathbb{R}^3$) by an application of the unit point forces at the origin of coordinates and oriented in the direction of coordinate axes.

As the closed-form expressions $\mathbf{U}(\mathbf{x})$ do not exist for all classes of these materials, and an efficient numerical procedure for evaluation of $\mathbf{U}(\mathbf{x})$, and even more of its derivatives, is not immediate, BEM is still not so popular for these materials as it is for isotropic materials and, thus, any progress in extending the scope of BEM applicability to these materials would be welcome.

For a better understanding of the context of the present work, the main contributions to the development of expressions of different kinds for $\mathbf{U}(\mathbf{x})$ suitable for implementation in 3D BEM codes will be briefly reviewed.

1.1. Fundamental solution for general anisotropic materials in 3D

With reference to general anisotropic elastic materials, working from the Fredholm expression of $\mathbf{U}(\mathbf{x})$ [5] obtained by the 3D Fourier transform, subseq contributions were aimed at obtaining an expression of $\mathbf{U}(\mathbf{x})$ as explicit and simple as possible. Lifshitz and Rozentsweig [6] applied the Cauchy residue calculus to a 1D integral obtained from the 3D Fourier integral, giving an explicit expression of $\mathbf{U}(\mathbf{x})$ in terms of the complex poles, roots of a sixth-order algebraic equation (called the Stroh eigenvalues at present), excluding degenerate cases with multiple poles from their calculation.

The application of the Stroh formalism to anisotropic elasticity (see Ting [7]) to evaluate $\mathbf{U}(\mathbf{x})$ and its derivatives in 3D has been shown to be a fruitful approach, leading to several substantial contributions in the 1970s, e.g. by Malén [8], expressing $\mathbf{U}(\mathbf{x})$ in terms of the normalized Stroh eigenvectors provided that all eigenvalues are distinct, and also more recently, without assuming the distinctness of the eigenvalues, by Nakamura and Tanuma [9] (expressing $\mathbf{U}(\mathbf{x})$ in terms of the Stroh eigenvalues and eigenvectors) and Ting and Lee [10] and Lee [11] (expressing $\mathbf{U}(\mathbf{x})$ in terms of the Stroh eigenvalues only). Also Wu's [12] generalization of the Stroh formalism to 3D elasticity has been shown to be fruitful in generating Green's functions of different kinds in a uniform way, although its full potential still needs to be fully explored.

DOI: 10.1002/nme

Recently, Lee [11] deduced new general analytical expressions of the first- and second-order derivatives of $\mathbf{U}(\mathbf{x})$ in terms of the Stroh eigenvalues only, which further develop expressions originally derived by Barnett [13].

Note, at this point, that the problem of finding a closed-form analytical expression of $\mathbf{U}(\mathbf{x})$ in terms of elastic stiffnesses for a general anisotropic elastic material appears to be equivalent to finding closed-form expressions for the roots of the above-mentioned sextic equation. According to the work of Head [14], no general solution is possible in radicals of this sextic equation, and therefore it seems that a fully closed-form expression of $\mathbf{U}(\mathbf{x})$ for general anisotropy will never be available.

BEM applications to anisotropic elastic materials started with the work of Wilson and Cruse [15], who implemented the expressions of $\mathbf{U}(\mathbf{x})$ and its first- and second-order derivatives in terms of a 1D integral over the unit circle [5, 6] and achieved an efficient numerical procedure by tabulating the values of $\mathbf{U}(\mathbf{x})$ and its derivatives (with respect to spherical angles) and finally by interpolating these values in BEM calculations. Although, apparently, for a long time this was the only satisfactory and widely used numerical procedure, e.g. Schclar [16], it requires large computer storage for tabulated values and may not provide sufficient accuracy in materials with a high degree of anisotropy.

A new numerical procedure for a direct evaluation of $\mathbf{U}(\mathbf{x})$ and its derivatives, which is more accurate and more efficient (in terms of both computer storage and time), was developed by Gray and co-workers [17–19] from expressions obtained by residue calculations [20], covering also the degenerate cases with multiple poles. Another 3D BEM implementation based on Wang's [21] residue calculations was developed by Tonon *et al*. [22].

Finally, let us mention that, to the best of the authors' knowledge, the explicit expressions of $\mathbf{U}(\mathbf{x})$ for general anisotropic materials obtained using the concepts of the Stroh formalism in [9–11] have not yet been implemented and validated in the BEM context.

1.2. Fundamental solution for transversely isotropic materials in 3D

Now, with reference to transversely isotropic elastic materials, the above-mentioned sextic equation can be solved in radicals [23, 24], and consequently the closed-form expressions of $\mathbf{U}(\mathbf{x})$ and its derivatives are possible. This feature represents a fundamental difference with respect to the above-discussed general anisotropy case and will be further exploited in the present work.

Whereas numerical approaches, such as modulation function interpolation [15, 16] or numerical solution of the sextic equation for different relative orientations of the source and field points [17–19], are the unique option for generally anisotropic materials where closed-form expressions are not available, it is expected that using a closed-form expression of $\mathbf{U}(\mathbf{x})$ for transversely isotropic materials will yield significant savings in computing time and a higher accuracy.

Without loss of generality, let the x_3-axis be the rotational-symmetry axis, and the x_1x_2-plane be the isotropy plane. Applying Voigt reduced notation [7], the elastic stiffnesses are represented by a symmetric and positive-definite matrix C_{IJ} $(I, J = 1, \ldots, 6)$. A transversely isotropic material is characterized by the following five elastic constants:

$$C_{1111} = C_{11}, \quad C_{3333} = C_{33}, \quad C_{1122} = C_{12}, \quad C_{1133} = C_{13}, \quad C_{2323} = C_{44} \tag{2}$$

It holds that $C_{1212} = C_{66} = (C_{11} - C_{12})/2$. Let

$$\triangle = \sqrt{C_{11}C_{33}} - C_{13} - 2C_{44} \tag{3}$$

DOI: 10.1002/nme

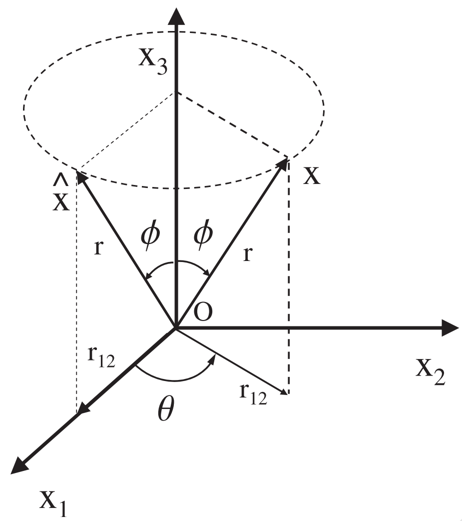

Figure 1. Points $\mathbf{x}$ and $\widehat{\mathbf{x}}$ in spherical coordinates associated with a transversely isotropic material.

Consider a point $\mathbf{x} \neq \mathbf{0}$ and a pair of orthogonal unit vectors $\mathbf{n}(\mathbf{x})$ and $\mathbf{m}(\mathbf{x})$, $\mathbf{n} \perp \mathbf{m}$, situated on the plane perpendicular to (the position vector) $\mathbf{x}$ so that $(\mathbf{n}, \mathbf{m}, \mathbf{x}/r)$, $r = |\mathbf{x}|$, form a right-handed triad. Let ϕ, $0 \leqslant \phi \leqslant \pi$, be the angle between the x_3-axis and vector $\mathbf{x}$, shown in Figure 1.

Several closed-form expressions of $\mathbf{U}(\mathbf{x})$ for a transversely isotropic material presented in the past have been obtained in different ways. Whereas Lifshitz and Rozentsweig [6], Kröner [25], Willis [26], Lejček [27] and Hu *et al*. [28] directly evaluated expressions obtained from the general formula of Fredholm [5], Elliot [29], Chen [30], Pan and Chou [31], Fabrikant [32], Hanson [33] and Loloi [34] applied the potential function approach, and Nakamura and Tanuma [9], Ting and Lee [10] and Lee [11] combined Fredholm's approach and Stroh formalism.

It will be instructive to relate, in what follows, the degeneracy cases (depending on the material properties and the direction of $\mathbf{x}$) observed in the expressions of $\mathbf{U}(\mathbf{x})$ for transversely isotropic materials obtained by the potential function approach with the classification of the fundamental elasticity matrix $\mathbf{N}(\mathbf{n}, \mathbf{m})$, in the framework of the Stroh formalism [7, 35].

The fundamental elasticity matrix $\mathbf{N}(\mathbf{n}, \mathbf{m})$ in the Stroh formalism is non-semisimple (having a double or a triple eigenvalue, and only two independent eigenvectors) if $\triangle = 0$ [23, 24]. It is not difficult to show that $\triangle = 0$ is equivalent to zero discriminant of the characteristic quadratic equation of the potential theory.

The case of $\phi = 0$ or π also leads to a non-semisimple matrix $\mathbf{N}(\mathbf{n}, \mathbf{m})$ [23, 24]. In these cases, the potential function approach may lead to division by zero in the expressions of $\mathbf{U}(\mathbf{x})$ and some specific arrangements have to be applied [31, 33, 34].

In the remaining cases, $\mathbf{N}(\mathbf{n}, \mathbf{m})$ is semisimple (having a double eigenvalue for a specific combination of elastic stiffnesses with C_{44}/C_{66}, giving a solution of the characteristic quadratic equation of the potential theory) or simple (having three different eigenvalues), and has three independent eigenvectors in any case. In these cases, $\triangle > 0$ and $\triangle < 0$, respectively, lead to real and complex solutions of the characteristic quadratic equation of the potential theory, which correspondingly produce real- and complex-variable expressions of $\mathbf{U}(\mathbf{x})$.

DOI: 10.1002/nme

Note that the complex-variable expressions of $\mathbf{U}(\mathbf{x})$ obtained by using the potential theory in the case $\triangle<0$ include complex functions, which are cumbersome for implementing in a BEM code and require very careful programming to keep their values in the same branch when multivaluedness arises [31]. Therefore, it is not a surprise that BEM results obtained by using these complex-variable expressions of $\mathbf{U}(\mathbf{x})$ for materials with $\triangle<0$ have not been published so far, at least to the knowledge of the present authors.

From the above-mentioned closed-form expressions of $\mathbf{U}(\mathbf{x})$, the expression deduced by Pan and Chou [31] is usually used in BEM codes; see Sáez *et al*. [36] and Loloi [34] for its BEM implementations and Ariza and Domínguez [37] for an expression of the hypersingular kernel in the traction BIE obtained from the second-order derivatives of $\mathbf{U}(\mathbf{x})$.

As discussed above, this solution [31] has several features that make its implementation covering all possible cases somewhat cumbersome: (i) expressions depending on the values of $\triangle$ (positive, negative or zero) and in particular its complex-variable character for $\triangle<0$; (ii) a loss of precision and/or a division by zero for $\phi=\pi$. Although the difficulty with the degeneracy problem at $\phi=\pi$ has been solved by Loloi [34] by means of an *ad hoc* approach (using the $\text{sign}(x_3)$ function), the mentioned features may still cause some difficulties in using this expression in further analytical deductions and in BEM development.

The aim of the present work is to obtain, and numerically test, completely general and closed-form real-variable expressions of $U_{ik}(\mathbf{x})$, its derivative $U_{ik,j}(\mathbf{x})$, and its corresponding stress Σ_{ijk} and traction $T_{ik}(\mathbf{x})$ solutions, valid for any transversely isotropic material. In Sections 2 and 3, a deduction of such an expression of $U_{ik}(\mathbf{x})$ introduced by Ting and Lee [10] is briefly revised for the sake of completeness and the necessary notation introduced. Section 4 presents new expressions for the associated solutions: $U_{ik,j}(\mathbf{x})$, Σ_{ijk} and $T_{ik}(\mathbf{x})$, obtained by differentiating this expression of $U_{ik}(\mathbf{x})$, which uphold all its advantages. The formulation of the Somigliana displacement identity, where $U_{ik}(\mathbf{x})$ and $T_{ik}(\mathbf{x})$ play the role of the integral kernels, with its free-term coefficient tensor is discussed in Section 5, where also a BEM implementation of this identity is presented. Finally, numerical tests, where the correctness of the expressions of $U_{ik}(\mathbf{x})$ and $T_{ik}(\mathbf{x})$ and of their implementation in a BEM code is verified, are presented in Section 6.

2. DISPLACEMENT FUNDAMENTAL SOLUTION FOR ANISOTROPIC MATERIALS

According to Malén [8] and Lothe [38], $\mathbf{U}(\mathbf{x})$ can be expressed in terms of the Barnett–Lothe tensor $\mathbf{H}(\mathbf{x})$ as

$$\mathbf{U}(\mathbf{x})=\frac{1}{4\pi r}\mathbf{H}(\mathbf{x}) \tag{4}$$

Thus, in the context of BIEs, $\mathbf{H}(\mathbf{x})$ represents the *characteristic* (or *modulation*) function of the displacement fundamental solution $\mathbf{U}(\mathbf{x})$. It is well known that $\mathbf{H}(\mathbf{x})$ can be evaluated in several ways [7, 9, 10], one option being given by the integral

$$\mathbf{H}(\mathbf{x})=\frac{1}{\pi}\int_{-\infty}^{+\infty}\boldsymbol{\Gamma}^{-1}(p)\,\mathrm{d}p \tag{5}$$

with the matrix

$$\boldsymbol{\Gamma}(p)=\mathbf{Q}+p(\mathbf{R}+\mathbf{R}^{\mathrm{T}})+p^2\mathbf{T} \tag{6}$$

DOI: 10.1002/nme

expressed in terms of a parameter p and the matrices $\mathbf{Q}$, $\mathbf{R}$ and $\mathbf{T}$ defined for an $\mathbf{x} \neq \mathbf{0}$ as

$$Q_{ij} = C_{ijk\ell} n_j n_\ell, \quad R_{ik} = C_{ijk\ell} n_j m_\ell, \quad T_{ik} = C_{ijk\ell} m_j m_\ell \tag{7}$$

where superscript T denotes the matrix transpose. Note that the matrices $\mathbf{Q}$ and $\mathbf{T}$ are symmetric and positive-definite matrices.

It can be shown that $\mathbf{H}(\mathbf{x})$ is independent of the choice of $\mathbf{n}$ and $\mathbf{m}$ on the plane perpendicular to $\mathbf{x}$ [7]. As follows from the above relations, $\mathbf{H}(\mathbf{x})$ is a symmetric and positive-definite matrix depending only on the direction of $\mathbf{x}$ but not on its magnitude, i.e. $\mathbf{H}(\mathbf{x}) = \mathbf{H}(\mathbf{x}/r)$, and fulfilling $\mathbf{H}(-\mathbf{x}) = \mathbf{H}(\mathbf{x})$. Hence, $\mathbf{U}(\mathbf{x})$ is also a symmetric positive-definite matrix and $\mathbf{U}(-\mathbf{x}) = \mathbf{U}(\mathbf{x})$.

Lifshitz and Rozentsweig [6] obtained, by applying the Cauchy residue theory, an expression of the integral in (5), which can be expressed in the following form:

$$\mathbf{H}(\mathbf{x}) = 2i \sum_{v=1}^{3} \frac{\hat{\mathbf{\Gamma}}(p_v)}{|\mathbf{\Gamma}(p_v)|'} \tag{8}$$

where $|\mathbf{\Gamma}(p)|$ is the determinant of $\mathbf{\Gamma}(p)$, $|\mathbf{\Gamma}(p)|' = \mathrm{d}|\mathbf{\Gamma}(p)|/\mathrm{d}p$, $\hat{\mathbf{\Gamma}}(p_v)$ is the adjoint matrix of $\mathbf{\Gamma}(p_v)$ defined by the relation $\mathbf{\Gamma}(p_v)\hat{\mathbf{\Gamma}}(p_v) = |\mathbf{\Gamma}(p_v)|I$, where I is the identity matrix, and $p_\alpha = \alpha_v + \mathrm{i}\beta_v$ $(v = 1, 2, 3)$ are the three complex roots with the positive-definite imaginary part $(\beta_v > 0)$ of the sextic algebraic equation (sometimes called Stroh eigenvalues):

$$|\mathbf{\Gamma}(p)| = 0 \tag{9}$$

It should be noted that the expression of $\mathbf{H}(\mathbf{x})$ in (8) is not valid for mathematically degenerate cases with repeated roots p_v, e.g. $p_1 = p_2$ or $p_1 = p_2 = p_3$.

Ting and Lee [10], starting from (8) and writing $\hat{\mathbf{\Gamma}}(p)$ as a polynomial of degree 4 in p:

$$\hat{\mathbf{\Gamma}}(p) = \sum_{n=0}^{4} p^n \hat{\mathbf{\Gamma}}^{(n)} \tag{10}$$

achieved a new general expression of $\mathbf{H}(\mathbf{x})$ valid for any kind of linearly elastic material:

$$\mathbf{H}(\mathbf{x}) = \frac{1}{|\mathbf{T}|} \sum_{n=0}^{4} q_n \hat{\mathbf{\Gamma}}^{(n)} \tag{11}$$

where the real coefficients q_n are expressed through fractions defined in terms of p_v, with no division by zero in the degenerate cases as happens with the expression of $\mathbf{H}(\mathbf{x})$ in (8).

A simplified expression of $\mathbf{H}(\mathbf{x})$ can be achieved for configurations, materials and some specific positions of $\mathbf{x}$ with respect to a material, for which (9) is a cubic equation with real coefficients in p^2. In this case the determinant $|\mathbf{\Gamma}(p)|$ is expressed using (6) as

$$|\mathbf{\Gamma}(p)| = |\mathbf{T}|(p^2 - p_1^2)(p^2 - p_2^2)(p^2 - p_3^2) \tag{12}$$

which leads to the following form of the sextic equation (9):

$$[p^4 + (g^2 - 2h)p^2 + h^2][p^2 + \beta_3^2] = 0 \tag{13}$$

g, h and β_3 being real and positive. The two roots p_1 and p_2 are pure imaginary or complex numbers, whereas the root p_3 is always a pure imaginary number.

DOI: 10.1002/nme

Then, applying (10) and (12) in (8), a simple expression in the form of (11) is obtained

$$\mathbf{H}(\mathbf{x}) = \frac{1}{|T|\xi}\left\{\frac{\zeta}{h\beta_3}\hat{\boldsymbol{\Gamma}}^{(0)} + \hat{\boldsymbol{\Gamma}}^{(2)} + \delta\hat{\boldsymbol{\Gamma}}^{(4)}\right\} \tag{14}$$

where the real and positive numbers ζ, δ and ξ defined as

$$\zeta = -\mathrm{i}(p_1 + p_2 + p_3) = g + \beta_3 \tag{15a}$$

$$\delta = -(p_1 p_2 + p_2 p_3 + p_3 p_1) = h + g\beta_3 \tag{15b}$$

$$\xi = \mathrm{i}(p_1 + p_2)(p_2 + p_3)(p_1 + p_3) = g(h + g\beta_3 + \beta_3^2) \tag{15c}$$

depend only on $p_1 + p_2$, $p_1 p_2$ and p_3. Thus, it is not necessary to evaluate individually all the roots of the sextic equation, and the final expression (14) is valid for both non-degenerate and degenerate cases. Explicit expressions for β_3, h and g can be determined from (9) and (13) by determining first the pure imaginary root $p_3 = \mathrm{i}\beta_3$ by an explicit formula for roots of cubic algebraic equations [10].

Finally, the following key results by Ting and Lee [10] (Section 4 therein) will be useful in the evaluation of $\mathbf{H}(\mathbf{x})$ presented in the next section. If $\mathbf{x}$ is situated on a plane of elastic symmetry, then, without loss of generality, one can assume that this plane coincides with a coordinate plane (applying a suitable rotation of the coordinate system if necessary), which implies the reduction of (9) to (13) and the vanishing of some components of $\mathbf{H}(\mathbf{x})$ (e.g. $H_{12}(\mathbf{x}) = 0$ and $H_{23}(\mathbf{x}) = 0$ if the plane $x_2 = 0$ is a plane of elastic symmetry).

3. DISPLACEMENT FUNDAMENTAL SOLUTION FOR TRANSVERSELY ISOTROPIC MATERIALS

Consider a transversely isotropic material as specified in (2). Any plane that contains the x_3-axis is a plane of elastic symmetry and, according to [10], form (12) of the sextic equation and the completely explicit expression of $\mathbf{H}(\mathbf{x})$ from (14) could be applied for any point $\mathbf{x}$.

The following procedure leads to a relatively simple and general expression of $\mathbf{H}(\mathbf{x})$. Let us define a vector

$$\widehat{\mathbf{x}} = (r_{12}, 0, x_3) \quad \text{where } r_{12} = \sqrt{x_1^2 + x_2^2} \tag{16}$$

Let $c = \cos\phi = x_3/r$ and $s = \sin\phi = r_{12}/r$, the angle $0 \leqslant \phi \leqslant \pi$ being shown in Figure 1. Then, defining $\mathbf{n} = (c, 0, -s)$ and $\mathbf{m} = (0, 1, 0)$, $[\mathbf{n}, \mathbf{m}, \widehat{\mathbf{x}}/r]$ forms a right-handed triad. Explicit expressions for the non-zero terms of

$$\mathbf{H}(\widehat{\mathbf{x}}) = \begin{pmatrix} H_{11} & 0 & H_{13} \\ 0 & H_{22} & 0 \\ H_{13} & 0 & H_{33} \end{pmatrix} \tag{17}$$

DOI: 10.1002/nme

can be obtained using (14)

$$
\begin{aligned}
H_{11} &= \frac{1}{C_{66}\beta_3} + \frac{C_{44}c^2 + C_{33}s^2}{C_{11}C_{44}gh} - \frac{f}{\xi} \\
H_{22} &= \frac{1}{C_{11}g} + \frac{f}{\xi} \\
H_{33} &= \frac{1}{gh}\left\{\frac{h+c^2}{C_{44}} + \frac{s^2}{C_{11}}\right\} \\
H_{13} &= \tilde{H}_{13}s
\end{aligned} \tag{18}
$$

where

$$
\begin{aligned}
\tilde{H}_{13} &= \frac{(C_{13}+C_{44})c}{C_{11}C_{44}gh} \\
\eta &= C_{11}C_{33} - C_{13}^2 - 2C_{13}C_{44} \\
\beta_3 &= \left\{\frac{C_{66}c^2 + C_{44}s^2}{C_{66}}\right\}^{1/2} \\
h &= \left\{c^4 + \frac{\eta s^2 c^2}{C_{11}C_{44}} + \frac{C_{33}s^4}{C_{11}}\right\}^{1/2} \\
g &= \left\{2(h+c^2) + \frac{\eta s^2}{C_{11}C_{44}}\right\}^{1/2} \\
\xi &= g(h + g\beta_3 + \beta_3^2) \\
f &= \frac{h+c^2}{C_{66}} + \frac{gh}{C_{66}\beta_3} + \frac{C_{33}s^2}{C_{11}C_{44}}
\end{aligned} \tag{19}
$$

β_3, h, g and ξ being positive dimensionless functions of c and s.

A general expression of the tensor $\mathbf{H}(\mathbf{x})$ for any $\mathbf{x}$, in terms of cos and sin functions of spherical angles ϕ and θ of $\mathbf{x}$, can be obtained from (17) and (18) by the following transformation of components of $\mathbf{H}(\widehat{\mathbf{x}})$:

$$H_{ik}(\mathbf{x}) = \Omega_{ia}\Omega_{kb}H_{ab}(\widehat{\mathbf{x}}) \tag{20}$$

where the rotation matrix $\mathbf{\Omega}$ is defined as

$$\mathbf{\Omega} = \begin{pmatrix} \cos\theta & -\sin\theta & 0 \\ \sin\theta & \cos\theta & 0 \\ 0 & 0 & 1 \end{pmatrix} \tag{21}$$

the angle $0 \leqslant \theta < 2\pi$ being shown in Figure 1. Note that transformation rule (20) with (21) for $\mathbf{H}(\mathbf{x})$ evaluation has been obtained by a small correction in the original formula given in Reference [10].

DOI: 10.1002/nme

Finally, bringing together Equations (4) and (17)–(21), an explicit and completely general expression for the fundamental solution $\mathbf{U}(\mathbf{x})$ in a transversely isotropic material is obtained. The form of this expression suitable for a computational implementation obtained by performing explicitly the transforms indicated in (20) is given in the Appendix, see (A1), where the presence of several zero components in $\mathbf{H}(\widehat{\mathbf{x}})$ and $\mathbf{\Omega}$ has provided simple and short expressions of the components of $\mathbf{H}(\mathbf{x})$.

4. TRACTION FUNDAMENTAL SOLUTION FOR TRANSVERSELY ISOTROPIC MATERIALS

Let $E_{ijk}(\mathbf{x})$ represent strains at $\mathbf{x}$ originated in the infinite elastic medium subjected to a unit point force in the k-direction at the origin of coordinates. Then,

$$E_{ijk}(\mathbf{x}) = \frac{1}{2}\left(\frac{\partial U_{ik}}{\partial x_j}(\mathbf{x}) + \frac{\partial U_{jk}}{\partial x_i}(\mathbf{x})\right) = \frac{1}{2}(U_{ik,j}(\mathbf{x}) + U_{jk,i}(\mathbf{x})) \tag{22}$$

Derivatives of the displacement fundamental solution appearing in (22) can be expressed in a form analogous to (4):

$$U_{ik,j}(\mathbf{x}) = \frac{\widehat{U}_{ik,j}(\mathbf{x})}{4\pi r^2} \tag{23}$$

where $\widehat{U}_{ik,j}(\mathbf{x})$ is the *characteristic* (or *modulation*) function, which depends only on the direction of $\mathbf{x}$ but not on its magnitude, i.e. $\widehat{U}_{ik,j}(\mathbf{x}) = \widehat{U}_{ik,j}(\mathbf{x}/r)$. Notice that $\widehat{U}_{ik,j}(\mathbf{x}) = \widehat{U}_{ki,j}(\mathbf{x})$ and $\widehat{U}_{ik,j}(-\mathbf{x}) = -\widehat{U}_{ik,j}(\mathbf{x})$.

Starting from the expression of $U_{ik}(\mathbf{x})$ given by (4) and (17)–(21) and directly performing differentiation leads to somewhat large expressions for $\widehat{U}_{ik,j}(\mathbf{x})$, which, additionally, when expressed in terms of coordinates of point $\mathbf{x}$, include terms of the type 'zero divided by zero' when $\mathbf{x}$ is placed on the x_3-axis. To avoid this problem, a trick analogous to that proposed by Ting and Lee [10] can be used here.

First, $\widehat{U}_{ik,j}(\widehat{\mathbf{x}})$ is evaluated by the above-described procedure. Then, considering that x_3 is the rotational-symmetry axis of the material, a general expression of $\widehat{U}_{ik,j}(\mathbf{x})$, in terms of cos and sin functions of spherical angles ϕ and θ of a point $\mathbf{x}$, is simply obtained by a transformation analogous to (20):

$$\widehat{U}_{ik,j}(\mathbf{x}) = \Omega_{ia}\Omega_{kb}\Omega_{jc}\widehat{U}_{ab,c}(\widehat{\mathbf{x}}) \tag{24}$$

Analytical evaluation of $\widehat{U}_{ik,j}(\widehat{\mathbf{x}})$ has been performed with the aid of the computer algebra software Mathematica [39]. The completely general and closed-form expressions of $\widehat{U}_{ik,j}(\widehat{\mathbf{x}})$ obtained are presented in a compact form suitable for computer implementation:

$$\begin{aligned}
&\widehat{U}_{11,1} = H'_{11}c - H_{11}s, \quad \widehat{U}_{12,2} = \tilde{H}_{12}s, \quad \widehat{U}_{11,3} = -H'_{11}s - H_{11}c\\
&\widehat{U}_{22,1} = H'_{22}c - H_{22}s, \quad \widehat{U}_{23,2} = \tilde{H}_{13}, \quad \widehat{U}_{22,3} = -H'_{22}s - H_{22}c\\
&\widehat{U}_{33,1} = H'_{33}c - H_{33}s, \quad \widehat{U}_{33,3} = -H'_{33}s - H_{33}c\\
&\widehat{U}_{13,1} = H'_{13}c - H_{13}s, \quad \widehat{U}_{13,3} = -H'_{13}s - H_{13}c
\end{aligned} \tag{25}$$

DOI: 10.1002/nme

where

$$
\begin{aligned}
\tilde{H}_{12} &= \frac{C_{33}}{C_{11}C_{44}gh} - \frac{\eta c^2 + C_{33}C_{44}s^2}{C_{11}C_{44}(h+c^2)}\left(\frac{1}{C_{11}gh} + \frac{g}{C_{66}\beta_3\xi}\right) + \frac{1}{\xi}\left(\frac{\eta - 2C_{33}C_{66}}{C_{11}C_{44}C_{66}} + \frac{C_{44}g}{C_{66}^2\beta_3}\right)\\
\beta_3' &= \frac{(C_{44}-C_{66})cs}{C_{66}\beta_3}\\
h' &= \frac{1}{h}\left(-2c^3 s + \frac{\eta cs}{C_{11}C_{44}}(c^2-s^2) + \frac{2C_{33}cs^3}{C_{11}}\right)\\
g' &= \frac{1}{g}\left(h' - 2cs + \frac{\eta cs}{C_{11}C_{44}}\right)\\
\xi' &= g(h' + g'\beta_3 + g\beta_3' + 2\beta_3\beta_3') + \frac{g'\xi}{g}\\
f' &= \frac{h'-2cs}{C_{66}} + \frac{1}{C_{66}\beta_3}\left(hg' + h'g - \frac{\beta_3' gh}{\beta_3}\right) + \frac{2C_{33}cs}{C_{11}C_{44}}\\
H_{11}' &= -\frac{\beta_3'}{C_{66}\beta_3^2} - \frac{C_{44}c^2 + C_{33}s^2}{C_{11}C_{44}gh}\left(\frac{h'}{h} + \frac{g'}{g}\right) + \frac{2(C_{33}-C_{44})cs}{C_{11}C_{44}gh} - \frac{1}{\xi}\left(f' - \frac{\xi' f}{\xi}\right)\\
H_{22}' &= -\frac{g'}{C_{11}g^2} + \frac{1}{\xi}\left(f' - \frac{\xi' f}{\xi}\right)\\
H_{33}' &= -\frac{1}{gh}\left(\frac{2cs}{C_{11}} + \frac{h'-2cs}{C_{44}}\right) - H_{33}\left(\frac{h'}{h} + \frac{g'}{g}\right)\\
H_{13}' &= \frac{C_{13}+C_{44}}{C_{11}C_{44}gh}\left(c^2 - s^2 - cs\left(\frac{h'}{h} + \frac{g'}{g}\right)\right)
\end{aligned}
\tag{26}
$$

Functions β_3', h', g', ξ', f' and H_{ik}' represent the first-order derivatives with respect to the angle ϕ of the corresponding functions defined in (18)–(19).

The remaining components of $\widehat{U}_{ik,j}(\widehat{\mathbf{x}})$ vanish:

$$\widehat{U}_{12,1} = \widehat{U}_{23,1} = \widehat{U}_{11,2} = \widehat{U}_{13,2} = \widehat{U}_{22,2} = \widehat{U}_{33,2} = \widehat{U}_{12,3} = \widehat{U}_{23,3} = 0 \tag{27}$$

It should be mentioned that in the original expression of $\widehat{U}_{12,2}(\widehat{\mathbf{x}})$, directly obtained by differentiating (20), the term $(H_{11} - H_{22})/s$ appeared, which would lead to zero divided by zero for points at the x_3-axis. This term, which has a finite limit value for $\phi \to 0$ or π, has been rewritten in the form $\tilde{H}_{12}s$, which is well defined for any point with $r > 0$.

DOI: 10.1002/nme

NME 2176

By applying the stress–strain constitutive law in matrix form, the stresses corresponding to the above fundamental solution are obtained as

$$\begin{Bmatrix} \Sigma_{11k} \\ \Sigma_{22k} \\ \Sigma_{33k} \\ \Sigma_{23k} \\ \Sigma_{13k} \\ \Sigma_{12k} \end{Bmatrix} = \mathbf{C} \begin{Bmatrix} E_{11k} \\ E_{22k} \\ E_{33k} \\ 2E_{23k} \\ 2E_{13k} \\ 2E_{12k} \end{Bmatrix} = \mathbf{C} \begin{Bmatrix} U_{1k,1} \\ U_{2k,2} \\ U_{3k,3} \\ U_{2k,3}+U_{3k,2} \\ U_{1k,3}+U_{3k,1} \\ U_{1k,2}+U_{2k,1} \end{Bmatrix} \tag{28}$$

where $\Sigma_{ijk}(\mathbf{x})$ represents the stress tensor σ_{ij} at $\mathbf{x}$ originated in the infinite elastic medium subjected to a unit point force in the k-direction at the origin of the coordinates. Again, it will be useful to write the stress fundamental solution in the form analogous to (4) and (23):

$$\Sigma_{ijk}(\mathbf{x}) = \frac{\widehat{\Sigma}_{ijk}(\mathbf{x})}{4\pi r^2} \tag{29}$$

where $\widehat{\Sigma}_{ijk}(\mathbf{x}) = \widehat{\Sigma}_{ijk}(\mathbf{x}/r)$. Notice that $\widehat{\Sigma}_{ijk}(\mathbf{x}) = \widehat{\Sigma}_{jik}(\mathbf{x})$ due to the symmetry of the stress tensor and $\widehat{\Sigma}_{ijk}(-\mathbf{x}) = -\widehat{\Sigma}_{ijk}(\mathbf{x})$.

By substituting expressions (23) and (29) into (28), it is easily seen that a relation analogous to (28) holds for the characteristic functions $\widehat{U}_{ik,j}(\mathbf{x})$ and $\widehat{\Sigma}_{ijk}(\mathbf{x})$ as well. Then, using expressions (25)–(27) directly gives the following closed-form expressions of $\widehat{\Sigma}_{ijk}(\widehat{\mathbf{x}})$:

$$\begin{aligned}
\widehat{\Sigma}_{111} &= C_{12}\tilde{H}_{12}s + C_{11}(H'_{11}c - H_{11}s) + C_{13}(-H'_{13}s - H_{13}c) \\
\widehat{\Sigma}_{221} &= C_{11}\tilde{H}_{12}s + C_{12}(H'_{11}c - H_{11}s) + C_{13}(-H'_{13}s - H_{13}c) \\
\widehat{\Sigma}_{331} &= C_{13}\tilde{H}_{12}s + C_{13}(H'_{11}c - H_{11}s) + C_{33}(-H'_{13}s - H_{13}c) \\
\widehat{\Sigma}_{131} &= C_{44}(-H'_{11}s - H_{11}c) + C_{44}(H'_{13}c - H_{13}s) \\
\widehat{\Sigma}_{232} &= C_{44}(-H'_{22}s - H_{22}c) + C_{44}\tilde{H}_{13} \\
\widehat{\Sigma}_{122} &= C_{66}\tilde{H}_{12}s + C_{66}(H'_{22}c - H_{22}s)s \\
\widehat{\Sigma}_{113} &= C_{13}(-H'_{33}s - H_{33}c) + C_{12}\tilde{H}_{13} + C_{11}(H'_{13}c - H_{13}s) \\
\widehat{\Sigma}_{223} &= C_{13}(-H'_{33}s - H_{33}c) + C_{11}\tilde{H}_{13} + C_{12}(H'_{13}c - H_{13}s) \\
\widehat{\Sigma}_{333} &= C_{33}(-H'_{33}s - H_{33}c) + C_{13}\tilde{H}_{13} + C_{13}(H'_{13}c - H_{13}s) \\
\widehat{\Sigma}_{133} &= C_{44}(H'_{33}c - H_{33}s) + C_{44}(-H'_{13}s - H_{13}c)
\end{aligned} \tag{30}$$

The remaining components of $\widehat{\Sigma}_{ijk}(\widehat{\mathbf{x}})$ vanish due to the fact that the plane $x_2 = 0$ is the symmetry or skew-symmetry plane of the elastic problem associated with a particular direction of the point force, namely

$$\widehat{\Sigma}_{121} = \widehat{\Sigma}_{231} = \widehat{\Sigma}_{112} = \widehat{\Sigma}_{222} = \widehat{\Sigma}_{332} = \widehat{\Sigma}_{132} = \widehat{\Sigma}_{123} = \widehat{\Sigma}_{233} = 0 \tag{31}$$

DOI: 10.1002/nme

Again, considering that x_3 is the rotational-symmetry axis of the material, a general expression of $\widehat{\Sigma}_{ijk}(\mathbf{x})$, in terms of cos and sin functions of spherical angles ϕ and θ of a point $\mathbf{x}$, is obtained by a transformation analogous to (24):

$$\widehat{\Sigma}_{ijk}(\mathbf{x}) = \Omega_{ia}\Omega_{jb}\Omega_{kc}\widehat{\Sigma}_{abc}(\widehat{\mathbf{x}}) \tag{32}$$

The corresponding traction fundamental solution $T_{ik}(\mathbf{x})$ associated with the unit normal vector $\mathbf{n}(\mathbf{x})$ is directly obtained from $\Sigma_{ijk}(\mathbf{x})$ by applying the Cauchy lemma:

$$T_{ik}(\mathbf{x}) = \Sigma_{ijk}(\mathbf{x})n_j(\mathbf{x}) \tag{33}$$

The main advantage of the above-presented expressions for $U_{ik,j}(\mathbf{x})$, $\Sigma_{ijk}(\mathbf{x})$ and $T_{ik}(\mathbf{x})$ in comparison with the previous expressions of other authors [31, 34] is that they are completely general real-variable expressions, valid for any combination of material parameters and any position of the evaluation point.

For a direct and efficient computational implementation of the obtained expressions of $\widehat{U}_{ik,j}(\mathbf{x})$ and $\widehat{\Sigma}_{ijk}(\mathbf{x})$ for any point $\mathbf{x} \neq \mathbf{0}$, the transforms indicated in (24) and (32) have been explicitly performed, producing compact and general expressions presented in the Appendix, which take advantage of the presence of many zero components in $\widehat{U}_{ik,j}(\widehat{\mathbf{x}})$ and $\widehat{\Sigma}_{ijk}(\widehat{\mathbf{x}})$. It has been numerically verified that, in terms of computational time, expressions (A2) and (A3) are significantly more efficient than their counterparts (24) and (32).

Finally, it should be mentioned that the reason for presenting in an explicit way expressions of the derivatives of the displacement fundamental solution and not only of the stress fundamental solution is the fact that BEM programmers sometimes prefer to use the first one instead of the second, and also the fact that these expressions are applied to second-order derivatives of the displacement fundamental solution for the deduction of the Somigliana stress identity.

5. BOUNDARY INTEGRAL EQUATION: FORMULATION AND NUMERICAL SOLUTION

5.1. Somigliana displacement identity

Consider a linearly elastic transversely isotropic solid $\Omega \subset \mathbb{R}^3$ with a bounded piecewise smooth Lipschitz boundary $\Gamma = \partial\Omega$.

Starting from the second Betti theorem of reciprocity of work, taking the fundamental solution as the auxiliary elastic state, and then applying the limit to the boundary, the Somigliana displacement identity, also called displacement BIE (u-BIE), is obtained [1–3]:

$$C_{ik}(\mathbf{x}')u_i(\mathbf{x}') + \int\!\!\!\!\!\!-_{\Gamma} T_{ik}(\mathbf{x},\mathbf{x}')u_i(\mathbf{x})\,\mathrm{d}S(\mathbf{x}) = \int_{\Gamma} U_{ik}(\mathbf{x}-\mathbf{x}')t_i(\mathbf{x})\,\mathrm{d}S(\mathbf{x}) \tag{34}$$

where $C_{ik}(\mathbf{x}') = \delta_{ik}$ for $\mathbf{x}' \in \Omega$, $C_{ik}(\mathbf{x}') = 0$ for $\mathbf{x}' \in \mathbb{R}^3 \backslash (\Omega \cup \Gamma)$, $u_i(\mathbf{x})$ and $t_i(\mathbf{x})$ are, respectively, are boundary displacements and tractions, $T_{ik}(\mathbf{x},\mathbf{x}')$ and $U_{ik}(\mathbf{x}-\mathbf{x}')$, represent respectively, the traction fundamental solution (associated with the unit outward normal vector $\mathbf{n}(\mathbf{x})$, $\mathbf{x} \in \Gamma$) and the displacement fundamental solution at the field point $\mathbf{x}$ due to the unit point force applied at the source point $\mathbf{x}'$. The strongly singular integral on the left-hand side is evaluated in the Cauchy principal value sense, whereas the weakly singular integral on the right-hand side is evaluated as an improper integral.

DOI: 10.1002/nme

The free-term coefficient tensor $C_{ik}(\mathbf{x}')$ for a boundary point $\mathbf{x}' \in \Gamma$ can be evaluated as

$$C_{ik}(\mathbf{x}') = -\lim_{\varepsilon \to 0_+} \int_{S_\varepsilon(\mathbf{x}') \cap \Omega} T_{ik}(\mathbf{x}, \mathbf{x}')\, \mathrm{d}S(\mathbf{x}) = -\oint_\Gamma T_{ik}(\mathbf{x}, \mathbf{x}')\, \mathrm{d}S(\mathbf{x}) \tag{35}$$

where $S_\varepsilon(\mathbf{x}')$ is a spherical surface of radius ε centred at $\mathbf{x}'$. Equation (35) implies that $C_{ij}(\mathbf{x}') = \frac{1}{2}\delta_{ij}$ for $\mathbf{x}'$ placed at a smooth part of Γ, whereas for $\mathbf{x}'$ at an edge or a corner its value depends on the local form and spatial orientation of Γ at $\mathbf{x}'$ and on the elastic material properties. An application of the Stokes theorem to obtain a more explicit formula for $C_{ik}(\mathbf{x}')$ at edge and corner points, advantageous for numerical (and possibly for analytic) computations, in a similar way as was previously done for isotropic materials [40], would also require an analogous decomposition of T_{ik}. In fact, such a decomposition is related to the Burgers formula [41], giving a displacement field originated by a unit dislocation loop. A generalization of the Burgers formula to general anisotropic materials was developed by Indenbom and Orlov [42], see also Lothe [38], and introduced in the framework of the symmetric Galerkin BEM by Rungamornrat [43] recently. According to these works, T_{ik} can be decomposed as

$$T_{ik}(\mathbf{x}, \mathbf{x}') = -\frac{\delta_{ik} n_j r_{,j}}{4\pi r^2} + D_{ij}(P_{jk}(\mathbf{x} - \mathbf{x}')) \tag{36}$$

where $r = |\mathbf{x} - \mathbf{x}'|$ and $r_{,j} = (x_j - x'_j)/r$, D_{ij} is the antisymmetric (tangential) differential operator defined by $D_{ij} = n_i(\mathbf{x})\partial_{x_j} - n_j(\mathbf{x})\partial_{x_i}$ and the weakly singular integral kernel P_{jk} can be expressed using a line integral similar to that appearing in (5). Then, the Stokes theorem, after the limit $\varepsilon \to 0$, leads to

$$C_{ik}(\mathbf{x}') = \frac{\Phi(\mathbf{x}')}{4\pi}\delta_{ik} + \int_{\partial S_1(\mathbf{x}', \Omega)} \varepsilon_{ijl} P_{jk}(\mathbf{x} - \mathbf{x}')\, \mathrm{d}x_l \tag{37}$$

where $\partial S_1(\mathbf{x}', \Omega)$ is the closed contour representing the boundary of the so-called characteristic surface $S_1(\mathbf{x}', \Omega)$ of Γ at $\mathbf{x}'$ (a polygon cut on the unit sphere $S_1(\mathbf{x}')$ by the tangential planes to Γ at $\mathbf{x}'$). $\Phi(\mathbf{x}')$ is the solid angle of $S_1(\mathbf{x}', \Omega)$ viewed from $\mathbf{x}'$. Formula (37) represents a generalization to anisotropic materials of the analogous formula for $C_{ik}(\mathbf{x}')$, in terms of $\Phi(\mathbf{x}')$ and regular line integrals over $\partial S_1(\mathbf{x}', \Omega)$, obtained previously for isotropic materials [40]. Note that the regular angular integrals over edges of $\partial S_1(\mathbf{x}', \Omega)$ can be evaluated numerically by standard quadratures. A study of the possibility of an analytical evaluation of these integrals would require a closed-form expression of P_{jk}, e.g. in a form similar to that shown for U_{ik} in Sections 2 and 3. To our knowledge, such a formula is not available at present.

Expressions of U_{ik} and T_{ik}, respectively, introduced in Equations (4) with (20) and (33) with (32) are considered in a cartesian coordinate system associated with the material (x_3-axis being the symmetry axis). An application of these expressions in a different coordinate system, cartesian or curvilinear, may be required at times. Rizzo and Shippy [44] analysed the corresponding transformations considering these fundamental solutions as two-point tensor functions. In the simpler case of a different cartesian coordinate system, it will be sufficient, first to evaluate these fundamental solutions in the material coordinate system, obtaining values U^*_{mn} and T^*_{mn}, and, second, to apply the standard transformation rule for second-rank tensors:

$$U_{ik} = Q_{im} Q_{kn} U^*_{mn}, \quad T_{ik} = Q_{im} Q_{kn} T^*_{mn} \tag{38}$$

DOI: 10.1002/nme

where $\mathbf{Q}$ is an orthogonal transformation matrix. It should be emphasized that the coordinates of the radius vector $\mathbf{x}-\mathbf{x}'$ between the field and source points and the normal vector appearing in the expressions of U^*_{mn} and T^*_{mn} should be given in the material coordinate system.

5.2. Boundary element method

The above-introduced expressions of U_{ik} and T_{ik} have been implemented in a 3D collocational BEM code (written in Fortran 90) for the numerical solution of u-BIE (34). The main features of the present BEM code [45] are as follows: (i) 9-node Lagrangian quadrilateral boundary elements with quadratic shape functions; (ii) a numerical evaluation of regular integrals by 8×8 Gaussian quadrature with adaptive subdivision of elements in the case of quasi-singular integrals [46]; (iii) the polar coordinate transformation applied to a numerical evaluation of weakly singular integrals with the integral kernel U_{ik}; (iv) the rigid-body-motion procedure applied to a numerical evaluation of the sum of the free-term coefficient tensor C_{ik} and the Cauchy principal value integral with the integral kernel T_{ik}.

6. NUMERICAL TESTS

The primary means of providing confidence in the correctness of the expressions of the displacement fundamental solution U_{ik} and traction fundamental solution T_{ik} introduced in the present work and also of their implementation in the present BEM code will be their application in the numerical solution of u-BIE (34) by this code.

Numerical results for problems in transversely isotropic elastic solids with known analytical solutions [47], coinciding with some problems solved by other authors [15, 34], except for the case with $\triangle<0$, where no previous numerical results by other authors have been found in the literature, will be studied.

For the purpose of comparison with expressions of U_{ik} and T_{ik} studied in the present work, the expression of U_{ik} due to Loloi [34] and an explicit expression of T_{ik} deduced by us, working from Loloi's expression of U_{ik}, have also been implemented in the BEM code. It can be mentioned that no final explicit expression of T_{ik} was given in Reference [34]. Note also that 4-node linear boundary elements were used in Reference [34], whereas 9-node quadratic boundary elements have been used in the present BEM code.

6.1. Example 1

Let Ω be an elastic transversely isotropic cube whose sides of length ℓ are parallel to coordinate axes, with the x_3-axis being the rotational-symmetry axis. Consider now this cube subjected to a simple tension. The elastic properties used in this example are given in Table I. The properties of Material 1 (with $\triangle>0$) and Material 2 (with $\triangle=0$) have been taken from Loloi [34], with the aim of comparing the numerical results obtained by using the expressions deduced from the original work of Pan and Chou [31] and those obtained here, starting from the work of Ting and Lee [10], both implemented in the present BEM code. Material 3 (with $\triangle<0$) is a hexagonal crystal of zinc.

In the BEM model used, the cube boundary is discretized by six elements, one element per cube side. Three load cases with normal stresses in the coordinate axes directions have been solved, with the symmetry boundary conditions applied at coordinate planes. Although an implicit symmetry can be applied for this example [34], the explicit symmetry was used here.

DOI: 10.1002/nme

Table I. Elastic properties considered in Example 1, values given in 10^6 psi.

Constants	Material no. 1 ($\triangle>0$)	Material no. 2 ($\triangle=0$)	Material no. 3 ($\triangle<0$)
C_{11}	49.40	49.40	23.35
C_{12}	34.60	34.60	4.96
C_{13}	9.70	9.70	7.27
C_{33}	38.10	38.10	8.85
C_{44}	14.20	16.84	5.55

Table II. Results of Example 1, Material no. 1 ($\triangle>0$).

Load direction	Displacements	Analytical solution	Present solution	Solution using [34]
x_3	u_1/u_3^e	−0.1154762	−0.1154762	−0.1154762
	u_2/u_3^e	−0.1154762	−0.1154762	−0.1154762
	u_3/u_3^e	1.0000000	1.0000000	1.0000000
x_1	u_1/u_1^e	1.0000000	0.9999998	0.9999998
	u_2/u_1^e	−0.6846397	−0.6846395	−0.6846395
	u_3/u_1^e	−0.0802886	−0.0802886	−0.0802886
x_2	u_1/u_2^e	−0.6846397	−0.6846395	−0.6846395
	u_2/u_2^e	1.0000000	0.9999998	0.9999998
	u_3/u_2^e	−0.0802886	−0.0802886	−0.0802886

Numerical results in displacements for Materials 1 and 2 are shown in Tables II and III together with the results obtained using the expressions derived from Loloi [34] and implemented in the present BEM code. The differences between both numerical solutions and the analytical solution are almost negligible, as could be expected from the characteristic of the analytical solution, linear in displacements and constant in stresses. An analogous conclusion is also valid for Material 3, (results shown in Table IV), where only the results obtained using the expressions of U_{ik} and T_{ik} introduced in the present work are shown, as complex-variable expressions of U_{ik} are given for materials with $\triangle<0$ in Loloi [34].

6.2. *Example 2*

A prismatic rod subjected to an axial load, Figure 2(a), is considered. The elastic properties in the material coordinate system are defined by

$$E/E' = 2.0, \quad E/\mu' = 6.0, \quad v = 0.3, \quad v' = 0.4 \tag{39}$$

where E and v are Young's elastic modulus and the Poisson ratio associated with the isotropy plane, E' is Young's modulus along the rotational-symmetry axis, and μ' and v' are the shear modulus

DOI: 10.1002/nme

Table III. Results of Example 1, Material no. 2 ($\triangle = 0$).

Load direction	Displacements	Analytical solution	Present solution	Solution using [34]
x_3	u_1/u_3^e	−0.1154762	−0.1154762	−0.1154867
	u_2/u_3^e	−0.1154762	−0.1154762	−0.1154867
	u_3/u_3^e	1.0000000	1.0000000	1.0000306
x_1	u_1/u_1^e	1.0000000	0.9999998	0.9999943
	u_2/u_1^e	−0.6846397	−0.6846395	−0.6846325
	u_3/u_1^e	−0.0802886	−0.0802886	−0.0802905
x_2	u_1/u_2^e	−0.6846397	−0.6846395	−0.6846325
	u_2/u_2^e	1.0000000	0.9999998	0.9999943
	u_3/u_2^e	−0.0802886	−0.0802886	−0.0802905

Table IV. Results of Example 1, Material no. 3 ($\triangle < 0$).

Load direction	Displacements	Analytical solution	Present solution
x_3	u_1/u_3^e	−0.2567997	−0.2567997
	u_2/u_3^e	−0.2567997	−0.2567997
	u_3/u_3^e	1.0000000	0.9999999
x_1	u_1/u_1^e	1.0000000	1.0000000
	u_2/u_1^e	0.0582394	0.0582393
	u_3/u_1^e	−0.8693108	−0.8693107
x_2	u_1/u_2^e	0.0582394	0.0582393
	u_2/u_2^e	1.0000000	1.0000000
	u_3/u_2^e	−0.8693108	−0.8693107

and Poisson ratio at the planes perpendicular to, the plane of isotropy. The plane of isotropy is inclined 45° with respect to the plane x_1x_2, which coincides with one rod base (Figure 2(a)). A BEM model of one-fourth of the rod, symmetry boundary conditions having been considered at the planes x_1x_3 and x_2x_3, with 14 elements, three elements at each lateral side and one element at each extreme section, has been used. Tension has been applied at the extreme sections, whereas, the lateral sides have been traction free.

Numerical results in displacements and stresses at the points indicated in Figure 2(a) are presented in Table V and compared with analytical values. Numerical solutions, in displacements and stresses, obtained by expressions of U_{ik} and T_{ik} from the present work and from Reference [34]

DOI: 10.1002/nme

NME 2176

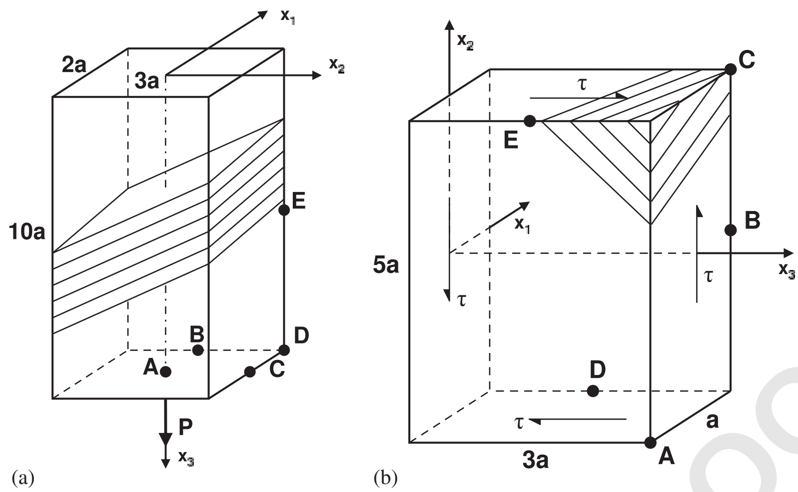

Figure 2. Transversely isotropic problem configurations with an inclined plane of isotropy for Examples 2 and 3.

Table V. Results of Example 2, transversely isotropic rod under axial tension.

Point	Results	u_1/u_3^e	u_2/u_3^e	u_3/u_3^e	$\sigma_{33}/\sigma_{33}^e$
A	Analytical solution	0.0000000	0.0000000	1.0000000	1.0000000
$(0, 0, 10a)$	Present solution	0.0000000	0.0000000	1.0000091	1.0000091
	Solution using [34]	0.0000000	0.0000000	1.0000091	1.0000091
B	Analytical solution	−0.0170732	0.0000000	1.0000000	1.0000000
$(a, 0, 10a)$	Present solution	−0.0170740	0.0000000	1.0000094	1.0000094
	Solution using [34]	−0.0170740	0.0000000	1.0000094	1.0000094
C	Analytical solution	0.0000000	−0.0670588	1.0000000	1.0000000
$(0, 1.5a, 10a)$	Present solution	0.0000000	−0.0670600	1.0000008	1.0000008
	Solution using [34]	0.0000000	−0.0670600	1.0000008	1.0000008
D	Analytical solution	−0.0164706	−0.0670588	1.0000000	1.0000000
$(a, 1.5a, 10a)$	Present solution	−0.0164714	−0.0670579	0.9999987	0.9999987
	Solution using [34]	−0.0164714	−0.0670579	0.9999987	0.9999987
E	Analytical solution	−0.0318182	−0.1295455	1.0000000	1.0000000
$(a, 1.5a, 5a)$	Present solution	−0.0318332	−0.1295392	1.0000002	1.0000002
	Solution using [34]	−0.0318332	−0.1295392	1.0000002	1.0000002
Centre	Analytical solution	0.0000000	0.0000000	1.0000000	1.0000000
$(0, 0, 5a)$	Present solution	0.0000000	0.0000000	1.0000107	1.0000107
	Solution using [34]	0.0000000	0.0000000	1.0000107	1.0000107

are coincident up to all 8 digits presented. The maximum relative errors defined by

$$\mathrm{err}(\sigma_{33}) = \frac{\sigma_{33}^n(\mathbf{x}) - \sigma_{33}^a}{\sigma_{33}^a}, \quad \mathrm{err}(u_i) = \frac{u_i^n(\mathbf{x}) - u_i^a(\mathbf{x})}{u_i^a(\mathbf{x})} \tag{40}$$

where the superscripts a and n refer to analytical and numerical results, respectively, are 0.00004 in stresses and 0.0004 in displacements.

Table VI. Results of Example 3, transversely isotropic rod under tangential stress.

Point	Result	u_1/u_3^e	u_2/u_3^e	u_3/u_3^e
A	Analytical solution	0.0990792	−0.1503137	1.0000000
$(-0.5a, -2.5a, 3a)$	Present solution	0.0990123	−0.1504005	1.0000161
	Solution using [34]	0.0990123	−0.1504005	1.0000161
B	Analytical solution	−0.5089075	−0.4758082	1.0000000
$(0.5a, 0, 3a)$	Present solution	−0.5084558	−0.4762378	1.0002009
	Solution using [34]	−0.5084558	−0.4762378	1.0002009
C	Analytical solution	0.1100334	−0.1669323	1.0000000
$(0.5a, 2.5a, 3a)$	Present solution	0.1101208	−0.1668616	0.9999395
	Solution using [34]	0.1101208	−0.1668616	0.9999395
D	Analytical solution	0.0679538	−0.1937795	1.0000000
$(0.5a, -2.5a, 1.5a)$	Present solution	0.0679590	−0.1937762	1.0000484
	Solution using [34]	0.0679590	−0.1937762	1.0000484
E	Analytical solution	0.0717356	−0.2045640	1.0000000
$(-0.5a, 2.5a, 1.5a)$	Present solution	0.0717414	−0.2045603	1.0000571
	Solution using [34]	0.0717414	−0.2045603	1.0000571

6.3. Example 3

A transversely isotropic rectangular parallelepiped, with elastic properties defined by (39), subjected to a shear load is considered, see Figure 2(b). The orientation of the coordinate system associated with the material is defined by the transformation matrix [34]

$$\mathbf{Q} = \begin{pmatrix} +0.7500 & +0.4330 & +0.5000 \\ -0.2403 & +0.8827 & -0.4040 \\ -0.6162 & +0.1828 & +0.7660 \end{pmatrix} \tag{41}$$

A BEM model of 10 elements, two at each lateral side and one at each extreme section, is applied. Due to the lack of symmetry and in order to avoid rigid body movements, displacements are prescribed at central points of each side except for the front ($x_1 = -a/2$) and back ($x_1 = a/2$) sides. Results in displacements at the points indicated in Figure 2(b) are presented in Table VI. Both numerical solutions are coincident up to all 8 digits shown, the maximum relative error, see definition in (40), being 0.0009, which confirms the correctness of the theoretical formulas used.

7. CONCLUSIONS

The present work deals with the closed-form expressions of the integral kernels $U_{ik}(\mathbf{x})$ and $T_{ik}(\mathbf{x})$ appearing in the Somigliana displacement identity for transversely isotropic elastic materials, and also of the related integral kernels $U_{ik,j}(\mathbf{x})$ and $\Sigma_{ijk}(\mathbf{x})$. The novel approach developed recently by Ting and Lee [10] yielded a closed-form expression of $U_{ik}(\mathbf{x})$ with the following unique features: (i) completely general and unique expressions valid for all possible configurations of material and relative positions of the source and field points; (ii) given by means of real functions (no difficulties with using complex functions with complex arguments which may require keeping values in the same branch when multivaluedness arises as in the expressions obtained from the

DOI: 10.1002/nme

potential theory [31, 34] in the case $\triangle<0$, see (3)); (iii) continuous transition with respect to a variation of material properties (the expressions obtained from the potential theory approach [31, 34] require two distinct expressions for the cases $\triangle\neq 0$ and $\triangle=0$); (iv) continuous transition with respect to relative positions of the source and field points (the sign function was introduced in the $U_{ik}(\mathbf{x})$ expression obtained from the potential theory [34] to cover both cases where $\phi\rightarrow 0$ or π); and (v) a straightforward and an efficient implementation in a BEM code.

These features have been upheld by the new closed-form expressions of $U_{ik,j}(\mathbf{x})$, $\Sigma_{ijk}(\mathbf{x})$ and $T_{ik}(\mathbf{x})$ obtained in the present work, working from the expression of $U_{ik}(\mathbf{x})$ due to Ting and Lee [10], after a revision of their final formula.

These expressions of $U_{ik}(\mathbf{x})$ and $T_{ik}(\mathbf{x})$ have been implemented in a 3D collocational BEM code and verified numerically by solving several examples with known analytical solution, obtaining high-accuracy results in all cases. All three cases with positive, zero and negative $\triangle$ have been solved, previous BEM results by other authors for the case $\triangle<0$ not being known in the literature. This work also represents, to our knowledge the first numerical verification of the correctness of the novel expression of U_{ik} due to Ting and Lee [10].

A proposal for an efficient numerical evaluation of the free-term coefficient tensor C_{ik} in the Somigliana displacement identity has also been given.

It should also be pointed out that the new closed-form expression for the tractions originated by a unit point force in the infinite transversal isotropic space, T_{ik}, can also be used in the context of the theory of dislocations [26, 38, 41, 42], where T_{ik} has a work-conjugated interpretation of the displacements originated by a unit infinitesimal dislocation loop in this space.

Finally, the present work is considered a starting point for deducing a new closed-form expression of the hypersingular kernel in the Somigliana stress identity, which could uphold the above-mentioned advantageous features of the expressions of U_{ik}, $U_{ik,j}(\mathbf{x})$, $\Sigma_{ijk}(\mathbf{x})$ and $T_{ik}(\mathbf{x})$ studied and which will be the topic of a forthcoming work.

APPENDIX: EXPRESSIONS OF $H_{ik}(\mathbf{x})$, $\widehat{U}_{ik,j}(\mathbf{x})$ AND $\widehat{\Sigma}_{ijk}(\mathbf{x})$

In this section, the expressions corresponding to (20), (24) and (32), suitable for a direct and efficient implementation in three-dimensional BEM codes are introduced.

For the sake of simplicity of the expressions presented below, the following notation conventions will be used: the quantities on the left-hand side are evaluated at point $\mathbf{x}$ and the quantities on the right-hand side at point $\widehat{\mathbf{x}}$, the symbols $\mathbf{x}$ and $\widehat{\mathbf{x}}$ being omitted, and $C=\cos(\theta)$ and $S=\sin(\theta)$.

Then, $H_{ik}(\mathbf{x})$ can be expressed in terms of $H_{ik}(\widehat{\mathbf{x}})$ as follows:

$$\begin{aligned}
H_{11} &= H_{11}C^2 + H_{22}S^2\\
H_{12} &= (H_{11} - H_{22})CS\\
H_{13} &= H_{13}C\\
H_{22} &= H_{22}C^2 - H_{11}S^2\\
H_{23} &= H_{13}S\\
H_{33} &= H_{33}
\end{aligned} \tag{A1}$$

DOI: 10.1002/nme

$\widehat{U}_{ik,j}(\mathbf{x})$ can be expressed in terms of $\widehat{U}_{ik,j}(\widehat{\mathbf{x}})$ as follows:

$$
\begin{aligned}
\widehat{U}_{11,1} &= \{\widehat{U}_{11,1}C^2 + (2\widehat{U}_{12,2} + \widehat{U}_{22,1})S^2\}C\\
\widehat{U}_{11,2} &= \{(\widehat{U}_{11,1} - 2\widehat{U}_{12,2})C^2 + \widehat{U}_{22,1}S^2\}S\\
\widehat{U}_{11,3} &= \widehat{U}_{11,3}C^2 + \widehat{U}_{22,3}S^2\\
\widehat{U}_{12,1} &= \{\widehat{U}_{12,2}S^2 + (\widehat{U}_{11,1} - \widehat{U}_{12,2} - \widehat{U}_{22,1})C^2\}S\\
\widehat{U}_{12,2} &= \{\widehat{U}_{12,2}C^2 + (\widehat{U}_{11,1} - \widehat{U}_{12,2} - \widehat{U}_{22,1})S^2\}C\\
\widehat{U}_{12,3} &= (\widehat{U}_{11,3} - \widehat{U}_{22,3})CS\\
\widehat{U}_{13,1} &= \widehat{U}_{13,1}C^2 + \widehat{U}_{23,2}S^2\\
\widehat{U}_{13,2} &= (\widehat{U}_{13,1} - \widehat{U}_{23,2})CS\\
\widehat{U}_{13,3} &= \widehat{U}_{13,3}C\\
\widehat{U}_{22,1} &= \{(\widehat{U}_{11,1} - 2\widehat{U}_{12,2})S^2 + \widehat{U}_{22,1}C^2\}C\\
\widehat{U}_{22,2} &= \{\widehat{U}_{11,1}S^2 + (2\widehat{U}_{12,2} + \widehat{U}_{22,1})C^2\}S\\
\widehat{U}_{22,3} &= \widehat{U}_{11,3}S^2 + \widehat{U}_{22,3}C^2\\
\widehat{U}_{23,1} &= (\widehat{U}_{13,1} - \widehat{U}_{23,2})CS\\
\widehat{U}_{23,2} &= \widehat{U}_{13,1}S^2 + \widehat{U}_{23,2}C^2\\
\widehat{U}_{23,3} &= \widehat{U}_{13,3}S\\
\widehat{U}_{33,1} &= \widehat{U}_{33,1}C\\
\widehat{U}_{33,2} &= \widehat{U}_{33,1}S\\
\widehat{U}_{33,3} &= \widehat{U}_{33,3}
\end{aligned}
\tag{A2}
$$

$\widehat{\Sigma}_{ijk}(\mathbf{x})$ can be expressed in terms of $\widehat{\Sigma}_{ijk}(\widehat{\mathbf{x}})$ as follows:

$$
\begin{aligned}
\widehat{\Sigma}_{111} &= \{\widehat{\Sigma}_{111}C^2 + (2\widehat{\Sigma}_{122} + \widehat{\Sigma}_{221})S^2\}C\\
\widehat{\Sigma}_{112} &= \{(\widehat{\Sigma}_{111} - 2\widehat{\Sigma}_{122})C^2 + \widehat{\Sigma}_{221}S^2\}S\\
\widehat{\Sigma}_{113} &= \widehat{\Sigma}_{113}C^2 + \widehat{\Sigma}_{223}S^2\\
\widehat{\Sigma}_{121} &= \{\widehat{\Sigma}_{122}S^2 + (\widehat{\Sigma}_{111} - \widehat{\Sigma}_{122} - \widehat{\Sigma}_{221})C^2\}S\\
\widehat{\Sigma}_{122} &= \{\widehat{\Sigma}_{122}C^2 + (\widehat{\Sigma}_{111} - \widehat{\Sigma}_{122} - \widehat{\Sigma}_{221})S^2\}C\\
\widehat{\Sigma}_{123} &= (\widehat{\Sigma}_{113} - \widehat{\Sigma}_{223})CS
\end{aligned}
$$

DOI: 10.1002/nme

$$
\begin{aligned}
\widehat{\Sigma}_{131} &= \widehat{\Sigma}_{131}C^2 + \widehat{\Sigma}_{232}S^2\\
\widehat{\Sigma}_{132} &= (\widehat{\Sigma}_{131} - \widehat{\Sigma}_{232})CS\\
\widehat{\Sigma}_{133} &= \widehat{\Sigma}_{133}C\\
\widehat{\Sigma}_{221} &= \{(\widehat{\Sigma}_{111} - 2\widehat{\Sigma}_{122})S^2 + \widehat{\Sigma}_{221}C^2\}C\\
\widehat{\Sigma}_{222} &= \{\widehat{\Sigma}_{111}S^2 + (2\widehat{\Sigma}_{122} + \widehat{\Sigma}_{221})C^2\}S\\
\widehat{\Sigma}_{223} &= \widehat{\Sigma}_{113}S^2 + \widehat{\Sigma}_{223}C^2\\
\widehat{\Sigma}_{231} &= (\widehat{\Sigma}_{131} - \widehat{\Sigma}_{232})CS\\
\widehat{\Sigma}_{232} &= \widehat{\Sigma}_{131}S^2 + \widehat{\Sigma}_{232}C^2\\
\widehat{\Sigma}_{233} &= \widehat{\Sigma}_{133}S\\
\widehat{\Sigma}_{331} &= \widehat{\Sigma}_{331}C\\
\widehat{\Sigma}_{332} &= \widehat{\Sigma}_{331}S\\
\widehat{\Sigma}_{333} &= \widehat{\Sigma}_{333}
\end{aligned}
\tag{A3}
$$

ACKNOWLEDGEMENTS

The present work has been carried out during the research stays of L. T. and J. E. O. at the University of Seville, respectively, supported by the Program ALFA, ELBENet Europe Latin-American Boundary Element Network, and the Program Juan de la Cierva of the Spanish Ministry of Education and Science. L. T. also acknowledges the support of the Junta de Andalucia (Project of Excellence No. TEP 1207). V. M. and F. P. have been supported by the Spanish Ministry of Education and Science through project TRA2005-06764.

REFERENCES

1. Baláš J, Sládek J, Sládek V. *Stress Analysis by Boundary Element Method*. Elsevier: Amsterdam, 1989.
2. París F, Cañas J. *Boundary Element Method*, *Fundamentals and Applications*. Oxford University Press: Oxford, 1997.
3. Aliabadi MH. *The Boundary Element Method*, *Volume 2*, *Applications in Solids and Structures*. Wiley: Chichester, 2002.
4. Fairweather G, Karageorghis A. The method of fundamental solutions for elliptic boundary value problems. *Advances in Computational Mathematics* 1998; **9**:69–95.
5. Fredholm I. Sur les équations de l'équilibre d'um corps solide élastique. *Acta Mathematica* 1900; **23**:1–42.
6. Lifshitz IM, Rozentsweig LN. Construction of the Green tensor for the fundamental equation of elasticity theory in the case of unbounded elastically anisotropic medium. *Zhurnal Eksperimental'noi i Teoreticheskoi Fiziki* 1947; **17**:783–791.
7. Ting TCT. *Anisotropic Elasticity Theory and Applications*. Oxford University Press: Oxford, 1996.
8. Malén K. A unified six-dimensional treatment of elastic Green's functions and dislocations. *Physica Status Solidi B* 1971; **44**:661–672.

DOI: 10.1002/nme

9. Nakamura G, Tanuma K. A formula for the fundamental solution of anisotropic elasticity. *Quarterly Journal of Mechanics and Applied Mathematics* 1997; **50**:179–194.
10. Ting TCT, Lee VG. The three-dimensional elastostatic Green's function for general anisotropic linear elastic solids. *Quarterly Journal of Mechanics and Applied Mathematics* 1997; **50**:407–426.
11. Lee VG. Explicit expression of derivatives of elastic Green's functions for general anisotropic materials. *Mechanics Research Communications* 2003; **30**:241–249.
12. Wu K. Generalization of the Stroh formalism to 3-dimensional anisotropic elasticity. *Journal of Elasticity* 1998; **51**:213–225.
13. Barnett DM. The precise evaluation of derivatives of the anisotropic elastic Green's functions. *Physica Status Solidi* (*b*) 1972; **49**:741–748.
14. Head AK. The Galois unsolvability of the sextic equation of anisotropic elasticity. *Journal of Elasticity* 1979; **9**:9–20.
15. Wilson R, Cruse T. Efficient implementation of anisotropic three dimensional boundary-integral equation stress analysis. *International Journal for Numerical Methods in Engineering* 1978; **12**:1383–1397.
16. Schclar NA. *Anisotropic Analysis Using Boundary Elements*. Computational Mechanics Publications: Southampton, MA, 1994.
17. Sales MA, Gray LJ. Evaluation of the anisotropic Green's function and its derivatives. *Computers and Structures* 1998; **69**:247–254.
18. Phan AV, Gray LJ, Kaplan T. On the residue calculus evaluation of the 3-D anisotropic elastic Green's function. *Communications in Numerical Methods in Engineering* 2004; **20**:335–341.
19. Phan AV, Gray LJ, Kaplan T. Residue approach for evaluating the 3D anisotropic elastic Green's function: multiple roots. *Engineering Analysis with Boundary Elements* 2005; **29**:570–576.
20. Dederichs PH, Liebfried G. Elastic Green's function for anisotropic cubic crystals. *Physical Review* 1969; **188**:1175–1183.
21. Wang CY. Elastic fields produced by a point source in solids of general anisotropy. *Journal of Engineering Mathematics* 1997; **32**:41–52.
22. Tonon F, Pan E, Amadei B. Green's functions and boundary element method formulation for 3D anisotropic media. *Computers and Structures* 2001; **79**:469–482.
23. Tanuma K. Surface-impedance tensors of transversely isotropic elastic materials. *Quarterly Journal of Mechanics and Applied Mathematics* 1996; **49**:29–48.
24. Barroso A, Mantič V, París F. Analysis of singular stresses in transversely isotropic multimaterial corners using explicit expressions of the orthonormalized eigenvectors new in the Stroh formalism. *Engineering Fracture Mechanics*, submitted.
25. Kröner E. Das Fundamentalintegral der anisotropen elastischen Differentialgleichungen. *Zeitschrift für Physik* 1953; **136**:402–410.
26. Willis JR. The elastic interaction energy of dislocation loops in anisotropic media. *Quarterly Journal of Mechanics and Applied Mathematics* 1965; **18**:419–433.
27. Lejček L. The Green function of the theory of elasticity in an anisotropic hexagonal medium. *Czechoslovak Journal of Physics* 1969; **B19**:799–803.
28. Hu TB, Wang CD, Laio JL. Elastic solutions of displacements for a transversely isotropic full space with inclined planes of symmetry subjected to a point load. *International Journal for Numerical and Analytical Methods in Geomechanics* 2007; DOI: 10.1002/nag.602
29. Elliot HA. Three-dimensional stress distributions in hexagonal aelotropic crystals. *Proceedings of the Cambridge Philosophical Society* 1948; **44**:522–533.
30. Chen WT. On some problems in transversely isotropic elastic materials. *Journal of Applied Mechanics* 1966; **33**:347–355.
31. Pan Y, Chou T. Point force solution for an infinite transversely isotropic solid. *Journal of Applied Mechanics* 1976; **98**:608–612.
32. Fabrikant VI. *Applications of Potential Theory in Mechanics. Selection of New Results*. Kluwer Academic Publishers: Dordrecht, 1989.
33. Hanson MT. Some observations on the potential functions for transverse isotropy in the presence of body forces. *International Journal of Solids and Structures* 1998; **35**:3793–3813.
34. Loloi M. Boundary integral equation solution of three-dimensional elastostatic problems in transversely isotropic solids using closed-form displacement fundamental solutions. *International Journal for Numerical Methods in Engineering* 2000; **48**:823–842.

35. Ting TCT. A modified Leknitskii formalism *à la* Stroh for anisotropic elasticity and classifications of the 6×6 matrix **N**. *Proceedings of the Royal Society A*: *Mathematical*, *Physical and Engineering Sciences* 1999; **455**:69–89.
36. Sáez A, Ariza MP, Domínguez J. Three-dimensional fracture analysis in transversely isotropic solids. *Engineering Analysis with Boundary Elements* 1997; **20**:287–298.
37. Ariza MP, Domínguez J. Boundary element formulation for 3D transversely isotropic cracked bodies. *International Journal for Numerical Methods in Engineering* 2004; **60**:719–753.
38. Lothe J. Disclocations in anisotropic media. In *Elastic Strain Fields and Dislocation Mobility*, Indenbom VL, Lothe J (eds). North-Holland: Amsterdam, 1992.
39. Wolfram S. *Mathematica*, *A System for Doing Mathematics by Computer*. Addison-Wesley: Redwood City, CA, 1991.
40. Mantič V. A new formula for the C-matrix in the Somigliana identity. *Journal of Elasticity* 1993; **33**:191–201.
41. Burgers JM. Some considerations on the field of stress connected with dislocations in a regular crystal lattice. *Proceedings*, *Koninklijke Nederlandse Akademie van Wetenschappen* 1939; **42**:293–378.
42. Indenbom VL, Orlov SS. Construction of Green's functions in terms of Green's function of lower dimension. *Journal of Applied Mathematics and Mechanics* 1968; **32**:414–420.
43. Rungamornrat J. A computational procedure for analysis of fractures in three dimensional anisotropic media. *Ph.D. Thesis*, The University of Texas, 2004.
44. Rizzo FJ, Shippy DJ. Some observations on Kelvin's solution in classical elastostatics as a double tensor field with implications for Somigliana integral. *Journal of Elasticity* 1983; **13**:91–97.
45. Ortiz JE, Cisilino AP. Boundary element method for J-integral and stress intensity factor computations in three-dimensional interface cracks. *International Journal of Fracture* 2005; **133**:197–222.
46. Lachat JC, Watson JO. Effective numerical treatment of boundary integral equations: a formulation for three-dimensional elastostatics. *International Journal for Numerical Methods in Engineering* 1976; **10**:991–1005.
47. Lekhnitskii SG. *Theory of Elasticity of an Anisotropic Body*. Mir Publishers: Moscow, 1981.

DOI: 10.1002/nme